ON THE EFFECTS OF FATIGUE PRECRACKING ON THE MICROSTRUCTURE AROUND PRECRACK IN 1TCT FRACTURE TOUGHNESS SPECIMEN OF F82H-IEA—H. Tanigawa (Japan Atomic Energy Research Institute), N. Hashimoto, M. A. Sokolov, and R. L. Klueh (Oak Ridge National Laboratory), and M. Ando (JAERI)

OBJECTIVE

The objective of this work is to observe the effects of fatigue precracking on the microstructure around the precrack in 1TCT fracture toughness specimen of F82H-IEA.

SUMMARY

1TCT fracture toughness specimens of F82H-IEA steel were fatigue precracked and sliced in specimen thickness wise for microstructure analysis around the precrack. The microstructure around the precrack was observed by optical microscopy (OM), scanning electron microscopy (SEM), orientation imaging microscopy (OIM), and transmission electron microscopy (TEM). TEM samples around the crack front were prepared by focused ion beam (FIB) processor. The fracture surfaces of tested 1TCT specimens were also observed. OM observation showed that the precrack penetration was straight in the beginning, and then tended to follow a prior austenite grain boundary and to branch into 2 to 3 directions at the terminal. SEM and OIM observations revealed that the both microstructures around the precracks and ahead of the precrack had turned into cell structure, which is the typical microstructure of fatigue-loaded F82H. TEM images and inverse pole figures obtained from the crack-front region confirmed this structure change. Possible mechanisms by which the precrack branching or the cell structure ahead of precracks affects fracture toughness were suggested.

PROGRESS AND STATUS

Introduction

In the current JAERI-DOE fusion collaboration program, the ductile-brittle transition temperature (DBTT) of the reduced-activation ferritic/martensitic steels (RAFs) is to be determined by the master curve (MC) method, in which the DBTT of ferritic steels is characterized in terms of fracture toughness reference temperature, T_o, as defined in the ASTM standard E1921. This method works out when the transition fracture toughness values follow the MC that is usually independent of the type of steels or the type of the specimens once the value is scaled in the proper manner.

The problem with F82H-IEA[1], one of the RAFs being examined in this collaboration, is that some fracture toughness values obtained by 1TCT specimens fell outside tolerance bands of the MC (Fig.1)[2]. There are two potential reasons that could cause this problem: (1) the heat treatment sensitivity of F82H-IEA, and (2) the fatigue precracking. In this study, the latter possibility was investigated.

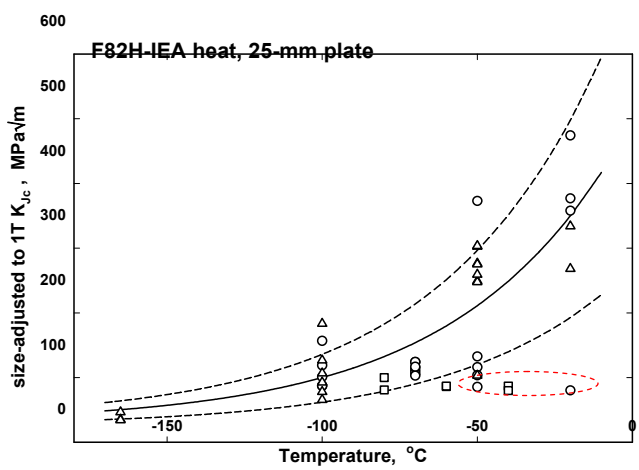

Fig. 1. The MC of F82H-IEA heat. Data points encircled by a broken red line indicate the toughness data which are below the lower tolerance bands of the MC.[2]

Fatigue microstructure of F82H was previously investigated [3,4] on low-cycle fatigue-fractured specimens, and the results revealed that the way that the fatigue crack propagated is that the cyclic

loading causes the lath structure to disappear and a cell structure forms, after which the fatigue crack propagates through the weakest portion of the cell structure. This fact indicates that fatigue precracking on a toughness specimen could induce the same type of microstructure into the region around the crack when the stress level is above the fatigue limit and propagate the crack through the weakest portion. On the other hand, even though ASTM standard E1921 defined the precracking procedure to minimize the effect of the plastic deformation zone on the fracture toughness value, the deformation range was just defined in the region where the stress level is above the yield stress. This could underestimate the effect of fatigue-induced deformation on ferritic/martensitic steels like F82H.

From this point of view, the effect of fatigue precracking on the toughness was investigated based on microstructure observations around the precrack induced in a 1TCT toughness specimen of F82H-IEA.

Experimental

1TCT specimens examined in this study were made from 25mm thick plate of F82H-IEA heat no. 9753, nominally Fe-7.5Cr-2W-0.15V-0.02Ta-0.1C, in wt%. The plate provided had been TIG welded and post weld heat treated at 993K for 1 hr [5]. The specimens were machined in L-T orientation such that loading will be in rolling direction and crack will propagate in transverse direction, and those were precracked as defined in ASTM standard E1921. A precracked and untested specimen was cut by EDM for microstructure examination around the precrack. It was then sliced in specimen thickness wise into 2.5mm thick pieces as shown in Fig.2. Each piece was mechanically polished to remove the EDM-affected zone, and then polished with SiC colloid to remove the effect of mechanical polishing. No electro-polishing was performed in order to conserve the region around the precrack. Fractured 1TCT specimens which showed various fracture toughness values were selected for fracture surface observation. Another specimen was prepared from the grip area of a tested specimen that exhibited a low toughness value. This specimen was polished and etched to perform optical metallography on the section perpendicular to the rolling direction (in plate thickness wise, i.e., specimen thickness wise). This specimen was etched with 8% nitric acid and 1% hydrofluoric acid in water.

Surface observations were performed by optical microscopy (OM) and scanning electron microscopy (SEM) using FE-SEM (Philips XL30). An orientation image microscopy (OIM) system (Tex SEM Laboratories) was used to analyze the grain orientation distribution. The OIM analysis was performed with a resolution of 50 to 150 nm. The specimens for transmission electron microscopy (TEM) were fabricated utilizing the focused ion beam (FIB) processor (Hitachi FB-2000A) with a microsampling system at Japan Atomic Energy Research Institute (JAERI). Further information on the FIB fabrication and these TEM observations can be found in ref. 6.

Results and Discussion

Fig.3 shows the cross sectional OM microstructure through the plate thickness, obtained from one 1TCT specimen with low fracture toughness. The microstructure is uniform thorough the thickness, with no banded structure, as reported by Gelles et.al.[7]. This could indicate that the low-energy fracture has no relation to the band microstructure. Fig.3 shows the fracture surfaces of 1TCT specimens fractured at different conditions. Condition A is for specimens that were tested at 253K or 233K and exhibited low toughness; the value is below the lower tolerance bound of the MC (Fig.4(a) and (b)). Condition B is for a specimen that was tested at 253K and exhibited high toughness; the value is within the tolerance bound of the MC (Fig.4(c)). Condition C is for a specimen that was tested at 173K and exhibited the toughness with the value within the tolerance band of the MC, but the value itself is the same as condition A (Fig.4(d)). On all specimens, the precracked fracture

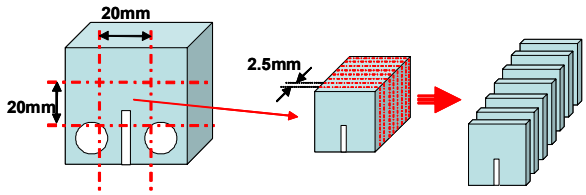

Fig. 2. Specimen preparation procedure for precrack observation on 1TCT specimen.

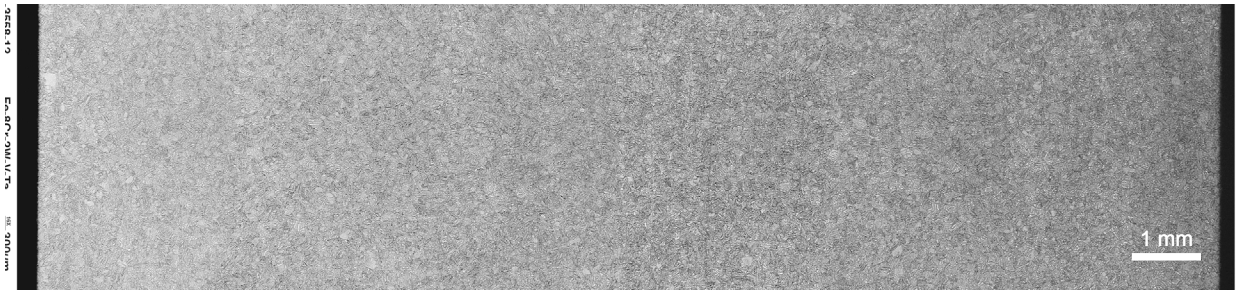

Fig. 3. Optical microstructure of cross section of F82H-IEA 25mm plate obtained from low-energy fractured 1TCT specimen.

(a) T_{test}=253K, K_{Jc}=80.2 MPa√m

(b) T_{test}=233K, K_{Jc}=87.3 MPa√m

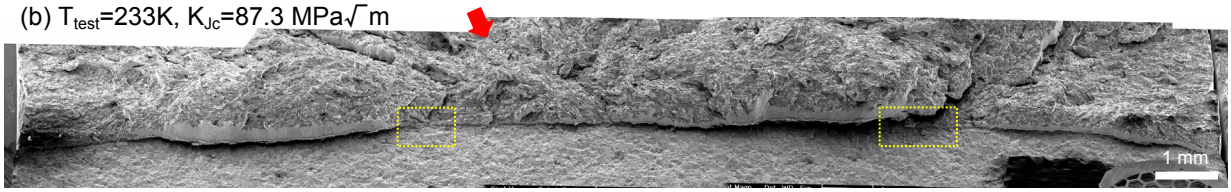

(c) T_{test}=253K, K_{Jc}=357.9 MPa√m

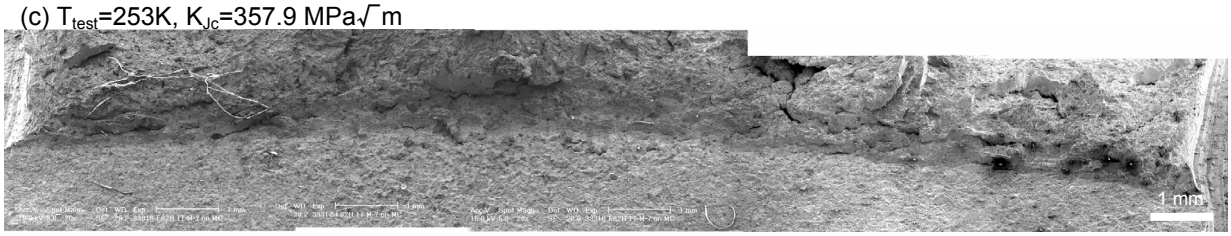

(d) T_{test}=173K, K_{Jc}=87.2 MPa√m

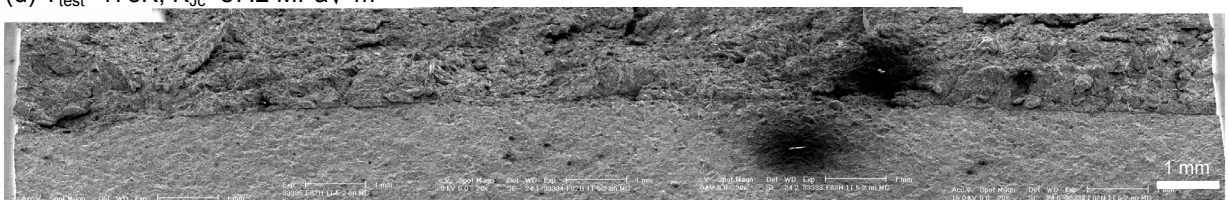

Fig. 4. SEM images of the fracture surface of 1TCT specimens which were tested at various conditions. Specimens were tilted 45 degrees. Images (a) and (b) were the fracture surfaces of the specimens which exhibited low toughness and those values were below the lower tolerance bound of the MC, (c) and (d) were the fracture surfaces of the specimens which exhibited the toughness which values were within the tolerance bound of the MC.

surfaces showed mostly flat and characterless surfaces, but the terminal of the precrack near the middle section showed intergranular fracture surfaces. On the specimen that exhibited low toughness and its value is below the lower tolerance bound of the MC (Fig.4(a), (b)), there is one apparent fracture initiation point (indicated with red arrow). Presence of this trigger point fits very well with premises of the MC methodology. There is also another indication that the fracture may start from very near the pre-crack front which shows inter-granular fracture (region indicated by yellow dashed square in Fig.4(a)), or start from branched crack which was observed beneath the main fracture plane (region indicated by yellow dashed square in Fig.4(b)). The magnified image (Fig.5) of the potential fracture starting point observed in Fig.4(a) shows the continuity from the fatigue pre-crack induced intergranular fracture surface. This might be interpreted as evidence that the fatigue crack which ends up as an intergranular fracture may cause the low-energy fracture.

It is also worth noting that these low-energy fracture surfaces have cracks parallel to the main crack. This might have a strong relationship to the branching of the fatigue precracks which were shown in Fig.6. Fig. 6 shows the pre-crack feature from a different region of specimen thickness. Numbers next to each image indicate the distance from the middle plane of the specimen thickness. These images indicate that the precracks initially propagated straight through the prior austenite grain (PAG), then started to follow the PAG boundary. At the terminal of the precrack, it branched into 2 or 3 cracks. This tendency is quite obvious in the middle section of the specimen.

To investigate the microstructure around the precrack in detail, SEM observations were made on the crack tip on the section +1.2mm from the center. Fig.7 shows back-scattered electron (BSE) images of the crack tip with a schematic drawing of the microstructure. The image shows that the fatigue precrack propagated through the PAG, but began to propagate along the PAG boundaries at its terminal. OIM images shown in Fig.8 suggest that the orientation distribution of the cell structure regions turned to dispersive, and they are different from what is observed on as-prepared F82H. These images indicate the presence of cell structure around the precrack, and this cell structure spread out for 60 μm ahead of crack tip into the direction the maximum shear stress was applied (Fig.8(c)).

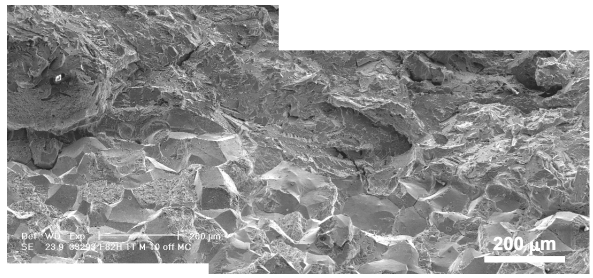

Fig. 5. Magnified image of the fracture initiation point near the precrack front observed in Fig.4(a).

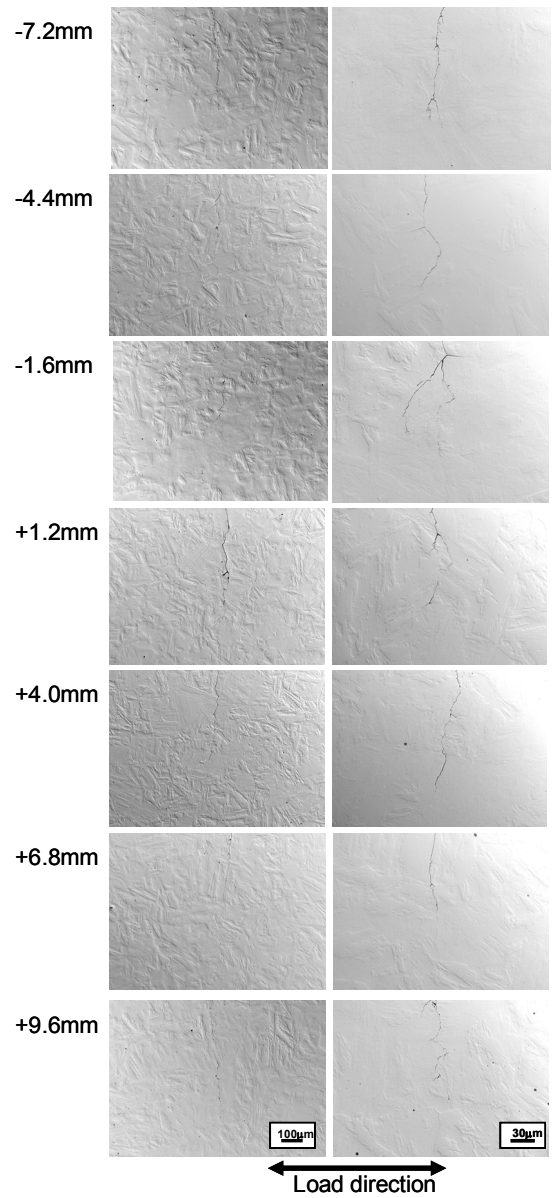

Fig. 6. Precrack features from the different thickness region of 1TCT specimen.

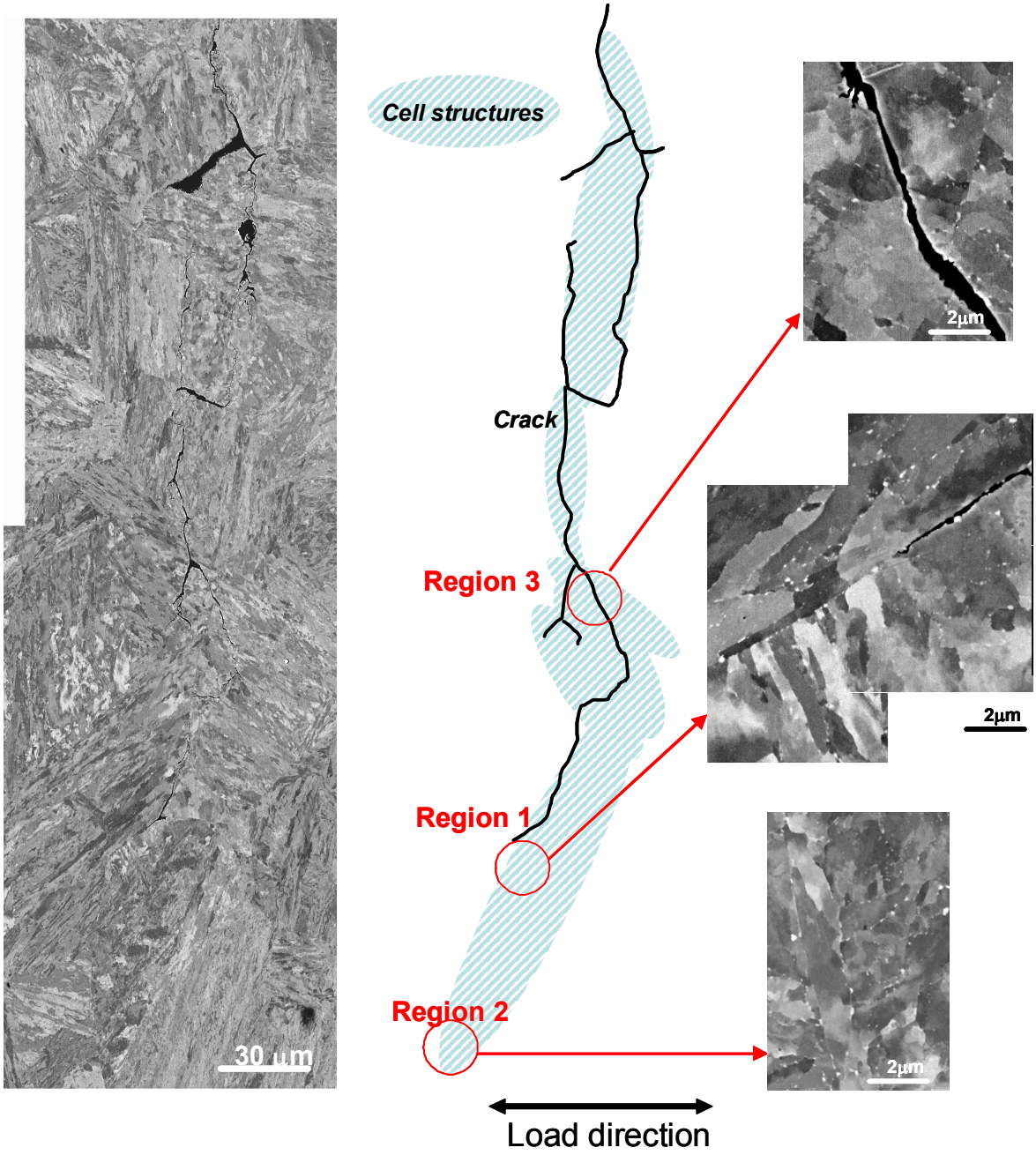

Fig. 7. The BSE images around the pre-crack tip with schematic drawing and magnified images of the microstructure. The specimen was prepared from the section 1.2mm from the middle plane of the 1TCT specimen thickness.

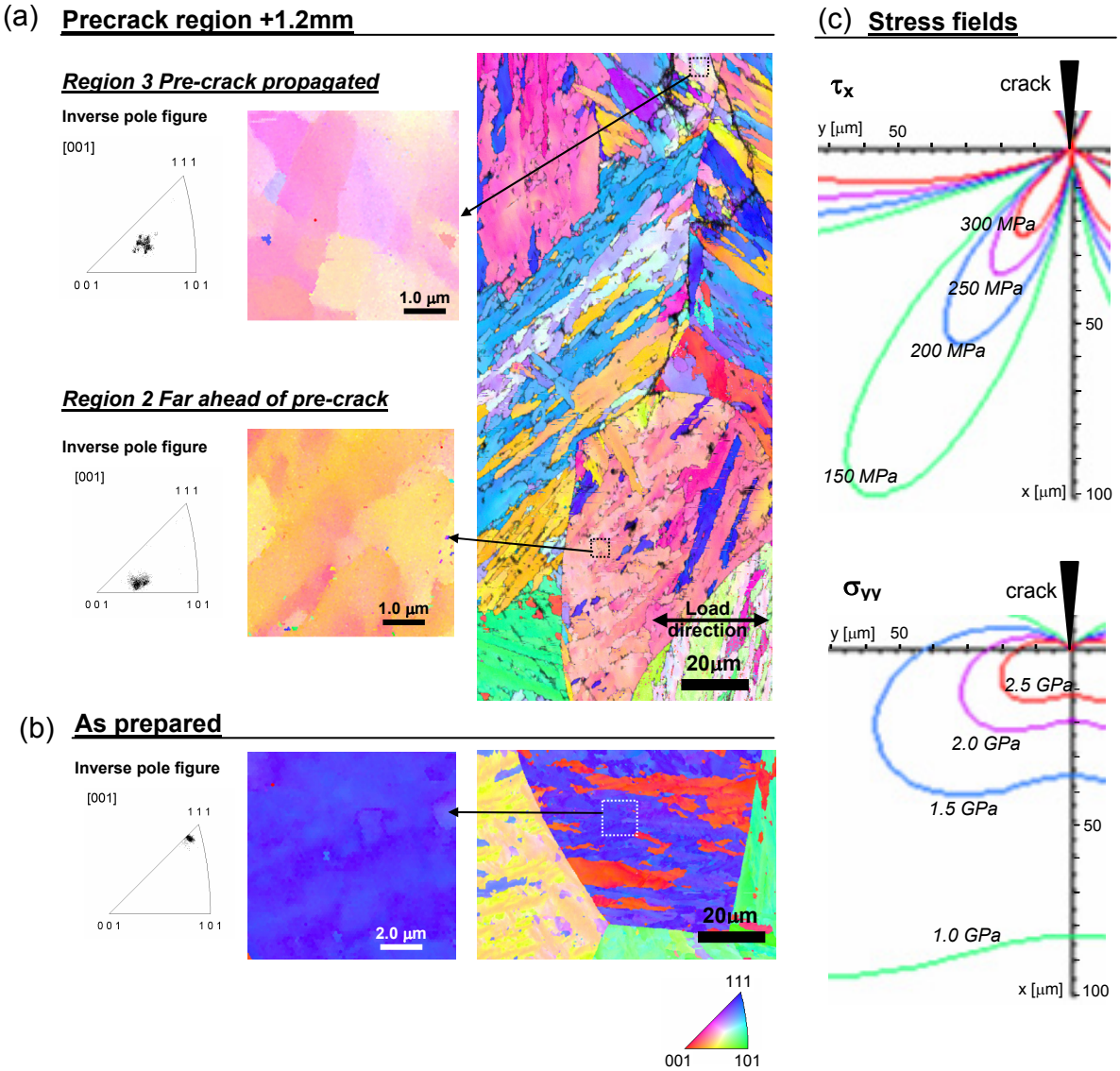

Fig. 8. The OIM images around the precrack tip (a), compared with the as-prepared images (b). Orientation distribution became dispersive as the color variation per unit area increased. Magnified OIM images obtained from precrack propagated region (region3) and ahead of precrack (region2) and as-prepared specimen are also shown with inverse pole figures (IPF) obtained from each magnified area. The calculated stress fields (τ_{xy}, σ_{yy}) for Mode I in a linear elastic, isotropic material is shown in (c) for comparison. No plastic deformation was taken into account. Stress intensity level that was used in the calculation (K = 22.8 MPa$\sqrt{m}$) is the condition at the end of precracking (1TCT, a/W=0.525, P=1270 kg).

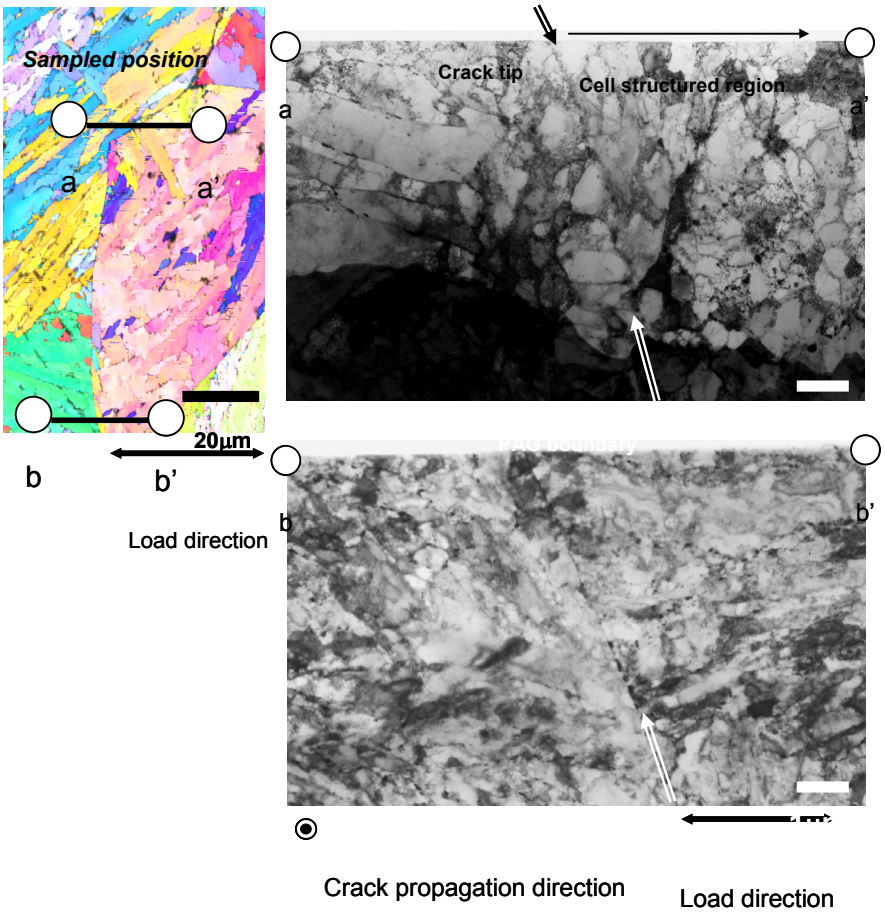

Fig. 9. TEM images of the microstructure at the fatigue precrack tip (a - a'), and the precrack front (b - b').

TEM specimens were sampled from the crack tip region (region 1 in Fig.8) and the region ahead of the crack tip (region 2 in Fig.8) by FIB processor (Fig.9).The specimen sampled from region 2 buckled while thinning, and this indicated the presence of residual stress on this region. Both TEM images confirm the presence of cell structure in each region. It is also worth noting the difference of microstructure between the right side and left side of the PAG boundary in region 1, i.e., the cell structure is distinctive in the right side of the PAG, but the lath structure is still observed on the left side of the PAG, and the crack is propagating along this PAG boundary in the middle of the image.

Fatigue fracture process on F82H-IEA was reported previously [3,4]; i.e., (1) the cell structure is induced in early cycle and then (2) a new cell structure is developed along the PAG boundary, and (3) the cracks propagate thorough the new cell structure cell along the PAG boundary.

Based on this, the fatigue pre-crack development could be interpreted as follows (Fig. 10):

(1) Fatigue-induced cell structure was developed in front of the notch, and the fatigue crack was formed.
(2) While the stress level was high, the fatigue cell structure was induced in front of the crack in a relatively wide range, and the crack continuously propagated in a straight line (Fig.10(a)).
(3) As the stress level was lowered as the crack developed, the fatigue cell structure began to form preferentially in the direction that the maximum shear stress was applied. (Fig.10(b))
(4) The crack began to propagate abruptly, i.e., the crack stopped until the cell structure was developed anisotropically ahead of the crack, then propagated through the weakest region in the developed cell structure, which is usually the PAG boundary. (Fig.10(c))
(5) Processes (3) and (4) were repeated until the fatigue loading was stopped.

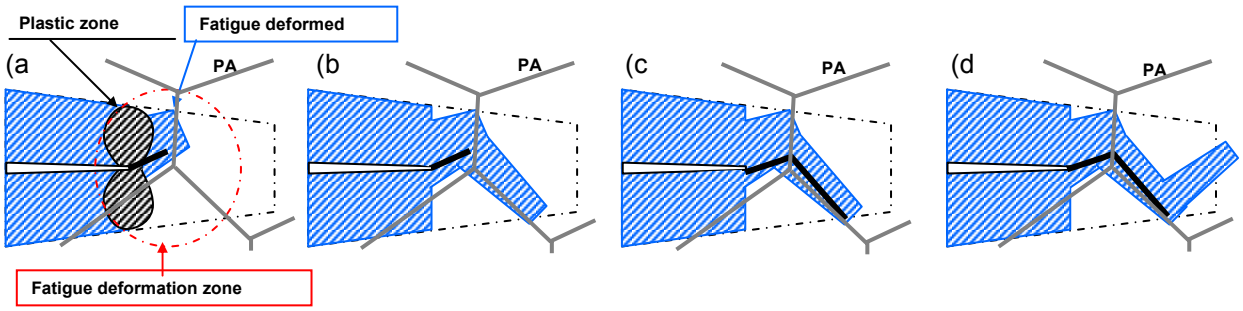

Fig. 10. Schematic drawing of precrack microstructure propagation.

This indicates that if the fatigue precracking process was stopped before the crack propagated thorough the cell structure developed in front of the precrack, then the specimen could have a locally weak (soft) region ahead of the crack (Fig.10(d)). The precrack branching is one of the cases, as the maximum shear stress is generally applied to the two directions ahead of the precrack (Fig.7(c)). This anisotropic cell structure formation in the maximum shear stress direction may cause the crack initiation without large-scale deformation, which was expected at those test temperatures that this low-energy fracture was observed. That is, the crack initiated in this cell structure region ahead of the precrack before the highest constraint region reached the critical condition to initiate the crack.

Although the cell structure could affect fracture toughness, the impact of the fatigue cell structure on the post-irradiation test might be small, because the local cell structure may be eliminated during irradiation. Further, most PIE will be performed at the temperature region where the specimen shows brittle fracture, as it was limited by the small specimen size. The irradiation microstructure development of fatigue cell structure should be examined to make sure of its effect.

The probability of the precrack branching and the scale of the cell structure anisotropically spread out ahead of the precrack tip could have a relation to the size of the PAG. F82H-IEA has large PAGs (~120μm), and consequently the packet, the area with similar crystal orientation, is generally large. This might allow the anisotropic cell structure development ahead of the precrack to occur over a longer distance, as shown in Fig.7 and Fig.8. Precrack branching could happen when the cell structure was equivalently developed enough for the crack propagation into the two directions where the maximum stress was loaded. On the other hand, if the PAG size is small, then the crystal orientation becomes less anisotropic even in a small range of area, and this would decrease the range of anisotropic cell structure development and the possibility of precrack branching. This implies the possibility that the low-toughness fracture value below the lower tolerance bound of the MC would not happen if the PAG size is small. Further fracture toughness experiments in view of this possibility will be conducted in near future.

SUMMARY AND CONCLUSIONS

The microstructure around the fatigue pre-crack of a 1TCT fracture toughness specimen of F82H-IEA steel was analyzed to investigate the cause of the low-energy fracture values that fell out of the tolerance band of the master curve. The pre-cracked 1TCT specimen was sliced through the thickness for various microstructural analyses. The fracture surfaces of tested 1TCT specimens were also observed. The following summarizes the observations and conclusions:

(1) The fracture surfaces of low-energy fractured specimen showed the presence of one apparent fracture initiation point, which fits very well with premises of the MC methodology, and it also showed the possibility that the fracture may start from the terminal of a precrack front which shows intergranular fracture or branched fracture.
(2) The precracks initially propagated straight through the PAG, then started to follow the PAG boundary, and at the terminal of the precrack, it branched into 2 or 3 cracks.

(3) The microstructure ahead of the precrack and around the precrack had turned into cell structure, which is the typical microstructure of fatigue-loaded ferritic/martensitic steels.
(4) It was suggested that the anisotropic cell structure formation ahead of precracks in the direction that the maximum shear stress was applied could cause the low-toughness fracture with values below the lower tolerance bound of the MC.
(5) The possibility that the large PAGs of F82H-IEA provoke the low toughness fracture was indicated.

Acknowledgements

All SEM and OIM analysis were performed at SHaRE Collaboration Research Center at Oak Ridge National Laboratory. This research was sponsored by the Japan Atomic Energy Research Institute and the Office of Fusion Energy Sciences, US Department of Energy under contract DE-AC05-96OR22464 with UT-Battelle.

References

[1] K. Shiba, M. Suzuki, and A. Hishinuma, J. Nucl. Mater. 233-237 (1996) 30.
[2] M. Sokolov et al., to be reported at next semiannual progress report (DOE/ER-0313/36, June 2004).
[3] T. Hirose, H. Tanigawa, M. Ando, and A. Kohyama, Mater. Trans. 43 (2001) 389.
[4] H. Tanigawa, T. Hirose, M. Ando, S. Jitsukawa, Y. Katoh, and A. Kohyama, J. Nucl. Mater. 307-311 (2002) 293.
[5] K. Shiba, R. L. Klueh, Y. Miwa, N. Igawa, and J. P. Robertson, DOE/ER-0313/ 28 (2000) 131.
[6] N. Hashimoto, H. Tanigawa, M. Ando, and M. A. Sokolov, in this progress report.
[7] D. S. Gelles and M. A. Sokolov, DOE/ER-0313/34 (2003) 49.